

A study of the influence of isotopic substitution on the melting point and temperature of maximum density of water by means of path integral simulations of rigid models.

Carl McBride,^a, Juan L. Aragones^a, Eva G. Noya,^b and Carlos Vega^{a†}

DOI: 10.1039/C2CP42393F

The melting point of ice I_h, as well as the temperature of maximum density (TMD) in the liquid phase, has been computed using the path integral Monte Carlo method. Two new models are introduced; TIP4PQ_D2O and TIP4PQ_T2O which are specifically designed to study D₂O and T₂O respectively. We have also used these models to study the “competing quantum effects” proposal of Habershon, Markland and Manolopoulos; the TIP4PQ/2005, TIP4PQ/2005 (D₂O) and TIP4PQ/2005 (T₂O) models are able to study the isotopic substitution of hydrogen for deuterium or tritium whilst constraining the geometry, while the TIP4PQ_D2O and TIP4PQ_T2O models, where the O-H bond lengths are progressively shortened, permit the study of the influence of geometry (and thus dipole moment) on the isotopic effects. For TIP4PQ_D2O - TIP4PQ/2005 we found a melting point shift of 4.9 K (experimentally the value is 3.68K) and a TMD shift of 6K (experimentally 7.2K). For TIP4PQ_T2O - TIP4PQ/2005 we found a melting point shift of 5.2 K (experimentally the value is 4.49K) and a TMD shift of 7K (experimentally 9.4K).

1 Introduction

Water molecules are composed of two hydrogen atoms and one oxygen atom (H₂O). One can substitute the hydrogen atom for isotopes of hydrogen: one can replace hydrogen for deuterium to form deuterium oxide (²H₂O, or D₂O), popularly known as “heavy water”, or with tritium, forming tritium oxide (³H₂O, or T₂O). These isotopically substituted forms of water differ in their physical properties, such as heat capacities (C_p), melting point (T_m), diffusion coefficients and the temperature of the maximum in density (TMD).

Within the Born-Oppenheimer approximation the “adiabatic surface”, or potential energy surface (PES) is unaffected by such isotopic substitutions; any shift in experimental properties is due to a different probability distribution of the different isotopes on the same PES, something that classical statistical mechanics is unable to describe. The quantum nature of the nuclei becomes increasingly relevant when dealing with light atoms, in particular hydrogen. For this reason the incorporation of nuclear quantum effects in water is germane. A complete quantum mechanical description of water would require the solution of the electronic Schrödinger equation for the electronic part of the Born-Oppenheimer approximation, in conjunction with, say, the path-integral formalism for the nuclear contribution¹⁻³. Such a “complete” solution is still in the far future⁴. An intermediate approach is to use an empirical potential in place of

the potential energy surface. A great many empirical potentials exist for water⁵ (perhaps more than for any other molecule), having varying degrees of success⁶. One recently proposed classical model has been shown to be capable of reproducing a good number of the thermodynamic and transport properties of water, namely the TIP4P/2005 model⁷.

Since in water nuclear quantum effects are significant^{8,9}, one must conclude that the parameters of these classical models implicitly include these quantum contributions. A path integral simulation of a model such as TIP4P/2005 would be inappropriate as it would lead to a “double-counting” of the nuclear quantum effects, so in view of this a variant of this model was developed; namely the TIP4PQ/2005 model¹⁰. It was found that an increase of 0.02e in the charge of the proton led to one of the most quantitative phase diagrams of water calculated to date¹¹.

Recently a very interesting suggestion has been put forward by Habershon, Markland and Manolopoulos¹², that of “competing quantum effects” in water; they have proposed that zero point fluctuations lead to a longer O-H bond length, and thus a larger dipole moment, making the water molecule “less” quantum, whereas on the other hand inter-molecular quantum fluctuations serve to weaken the hydrogen bonds, making the liquid as a whole more “quantum”. An analogous process almost certainly takes place upon isotopic substitution; the replacement of hydrogen with deuterium has two effects: on the one hand the hydrogen bond becomes stronger, since D is less delocalised, i.e. more classical, than H, whilst on the other hand replacing H with D reduces the intramolecular OH covalent bond length, which in turn decreases the dipole moment of the molecule,

^{0†} cvega@quim.ucm.es

^{0a} Departamento de Química Física, Facultad de Ciencias Químicas, Universidad Complutense de Madrid, 28040 Madrid, Spain

^{0b} Instituto de Química Física Rocasolano, Consejo Superior de Investigaciones Científicas, CSIC, Calle Serrano 119, 28006 Madrid, Spain

effectively reducing the strength of the hydrogen bond.

To study these competing quantum effects, and to examine the influence of isotopic substitution on both the melting point of ice I_h and the location of the temperature of maximum density (TMD) in the liquid, we studied the aforementioned TIP4PQ/2005 model along with two new models, specifically designed for simulations of D_2O and T_2O . Each of these models are both rigid and non-polarisable. Water molecules are, beyond a doubt, flexible in nature. Furthermore, it is known that the isotopic substitutions noticeably affect the vibrational properties of water¹³ and also that there is a degree of coupling between intermolecular and intramolecular modes. Since intramolecular vibrations are generally high frequency oscillations a quantum rather a classical description of these vibration would be desirable¹⁴. That said however, the thermodynamic properties of the condensed phases of water are largely dominated by the intermolecular hydrogen bond rather than by the intramolecular vibrations. For this reason an analysis of how far one can go in the description of isotopic effects on the TMD and melting point of water using rigid models is still pertinent. It will be shown that when the same model is used to study each of the isotopes of water the variation of the properties, although qualitatively correct, are overestimated. However, it will be shown that by simply shortening the O-D and O-T bond length with respect to that of O-H, then predictions of isotopic effects are in reasonable agreement with experimental results.

2 Methodology and simulation details

Recent experiments have indicated that the O-D bond length is shorter than the O-H bond length by $\approx 0.5\%$ ¹⁵. In view of this we have taken the TIP4PQ/2005 model, and also shortened the O-D distance by a similar amount (by 0.004\AA to be precise), resulting in the TIP4PQ_D2O model. The location of the negative charge (situated on the massless site M) was also shifted so as to maintain the same ratio of $d_{\text{OM}}/d_{\text{OH}}$ as in the original TIP4PQ/2005 model. On doing this the relative distances between the charges (responsible of the hydrogen bond strength) and the Lennard-Jones site (which controls the short range repulsive forces) remains unchanged, and provides a dipole to quadrupole ratio close to one, which has been shown to lead to a good phase diagram for TIP4P-like models¹⁶. We have also parameterised a model for T_2O (TIP4PQ_T2O) along the same lines. Given the paucity of experimental data for the O-T bond length in the liquid phase, we have taken the liberty of shortening the O-T bond length by 0.006\AA with respect to the H-O bond length, again maintaining the bond length ratio $d_{\text{OM}}/d_{\text{OH}}$. The resulting parameters are given in Table 1. It is worth reiterating that all of these models are rigid and non-polarisable. The path integral methodology for rigid rotors was employed and has been discussed in detail elsewhere¹⁷, and we shall restrict

Model	A (cm^{-1})	B (cm^{-1})	C (cm^{-1})
TIP4PQ/2005	27.432	14.595	9.526
TIP4PQ/2005 (D_2O)	15.262	7.303	4.939
TIP4PQ/2005 (T_2O)	11.211	4.877	3.398
TIP4PQ_D2O	15.390	7.365	4.981
TIP4PQ_T2O	11.353	4.939	3.441

Table 2 Rotational constants for each of the models.

ourselves to describing the most salient aspects of the work undertaken here. The NVM propagator¹⁸, exact for asymmetric tops, was used. The NVM propagator is based on the work of Müser and Berne for symmetric tops¹⁹. We used $P = 7$ Trotter slices, or “replicas”, for all simulations. In Table 2 the rotational constants for the various models are presented. Simulations of the liquid phase consisted of 360 molecules, and the ice I_h phase consisted of 432 molecules. The proton disordered configuration of ice I_h , having both zero dipole moment as well as satisfying the Bernal-Fowler rules²⁰ was obtained by means of the algorithm of Buch *et al.*²¹. The Lennard-Jones part of the potential was truncated at 8.5\AA and long range corrections were added. Coulombic interactions were treated using Ewald summation method. In the ice I_h phase the NpT ensemble was used, with anisotropic changes in the volume of the simulation box; each side being able to fluctuate independently. All simulations were performed at a pressure of 1 bar. A Monte Carlo cycle consists of a trial move per particle (the number of particles is equal to NP where N is the number of water molecules) plus a trial volume change in the case of NpT simulations.

2.1 Calculation of the melting point

Calculation of the melting point of ice I_h consists of three steps:

Step 1: The first step is to calculate the classical melting point for the model of interest. This consists in calculating the free energy of the solid phase via Einstein crystal calculations, followed by the addition of the residual entropy as calculated by Pauling²². To obtain the free energy of the fluid phase a thermodynamic path is constructed, making a connection to a Lennard-Jones reference fluid whose free energy is well known. Once the free energies of the fluid and solid phases of the classical system are known for a reference state thermodynamic integration is performed to obtain the temperature for which both phases have the same chemical potential (at standard pressure), i.e. the classical melting point. A thorough description of this procedure can be found in Ref.²³.

Step 2: At this classical melting point one then calculates the difference in chemical potential between ice I_h and water for the quantum system ($\Delta\mu$) via:

$$\frac{\Delta\mu}{k_B T} = \int_0^1 \frac{1}{\lambda'} \left[\left\langle \frac{K_{I_h}}{Nk_B T} \right\rangle - \left\langle \frac{K_{\text{liquid}}}{Nk_B T} \right\rangle \right] d\lambda' \quad (1)$$

Table 1 Parameters for TIP4PQ/2005 and the new TIP4PQ_D2O and TIP4PQ_T2O models. The distance between the oxygen and hydrogen sites is d_{OH} . The angle, in degrees, formed by hydrogen, oxygen, and the other hydrogen atom is denoted by H-O-H. The Lennard-Jones site is located on the oxygen with parameters σ and ϵ . The charge on the proton is q_H . The negative charge is placed in a point M at a distance d_{OM} from the oxygen along the H-O-H bisector.

Model	d_{OH} (Å)	\angle H-O-H	σ (Å)	ϵ/k_B (K)	q_H (e)	d_{OM} (Å)	p (Debye)
TIP4PQ/2005	0.9572	104.52	3.1589	93.2	0.5764	0.1546	2.388
TIP4PQ_D2O	0.9532	104.52	3.1589	93.2	0.5764	0.153954	2.378
TIP4PQ_T2O	0.9512	104.52	3.1589	93.2	0.5764	0.1536	2.373

where K represents the total kinetic energy, given by:

$$K = K_{tra} + K_{rot}, \quad (2)$$

where

$$K_{tra} = \frac{3NP}{2\beta} - \left\langle \frac{MP}{2\beta^2\hbar^2} \sum_{i=1}^N \sum_{t=1}^P (\mathbf{r}_i^t - \mathbf{r}_i^{t+1})^2 \right\rangle_{NpT}, \quad (3)$$

where P is the number of ‘beads’ and M is the molecular mass, and

$$K_{rot} = \left\langle \frac{1}{P} \sum_{t=1}^P \sum_{i=1}^N e_{rot,i}^{t,t+1} \right\rangle_{NpT} \quad (4)$$

where $e_{rot}^{t,t+1}$ is the rotational energy term of the NVM propagator (for details see Ref.¹⁸). The parameter λ' is defined so that the mass of each atom i of the system is scaled as $m_i = m_{i,0}/\lambda'$ where $m_{i,0}$ is the mass of atom i in the original system. The values of $m_{i,0}$ for H, D, T and O were taken from Ref.²⁴. On increasing the atomic masses by the factor $1/\lambda'$ the geometry and centre of mass of the molecule remains unchanged. Similarly the eigenvalues of the inertia tensor, and thus the energies of the asymmetric top appearing in the rotational propagator, are also scaled by this factor. Such a linear scaling particularly convenient for practical purposes. However, the same is not true for a transformation from, say, the TIP4PQ/2005 to TIP4PQ_D2O models, since the geometry and mass distribution varies between the models. Similarly there is no simple scaling for the values of the rotational constants A , B and C used in the calculation of the propagator. For this reason we perform the integration to infinite mass for each of the models, rather than perform a transformation between models. Eq. 1 embodies the idea that the phase that has the higher kinetic energy will also have the higher chemical potential and as a result will become less stable in the quantum system. Note that for the TIP4PQ/2005 model the melting point of the classical system is the same for H₂O, D₂O and T₂O since the melting point of a classical system is independent of the molecular mass. The integrand of Eq. 1 represents the transformation from H₂O (or D₂O or T₂O) to an infinitely massive molecule of water. This integral was evaluated using seven values of λ' between 1/7 and

1 (i.e. $\lambda' = 1, 6/7, 5/7, 4/7, 3/7, 2/7$, and $1/7$) by performing runs of about one million cycles at each value of λ' . We do not go beyond $\lambda' = 1/7$ due to the increased expense in the evaluation of the propagator, however, in Ref.¹¹ it is shown that the integral is well behaved down to $\lambda = 0$ for the case of the harmonic oscillator. Furthermore our direct coexistence simulations^{11,25} corroborate our melting point calculations, which take to be an indication that there is no ‘anomalous’ behaviour in the region between $\lambda' = 1/7$ and $\lambda' = 0$.

Step 3: Again using thermodynamic integration²³, the free energy of each phase of the quantum system is determined as a function of T :

$$\frac{G(T_2, p)}{Nk_B T_2} = \frac{G(T_1, p)}{Nk_B T_1} - \int_{T_1}^{T_2} \frac{H(T)}{Nk_B T^2} dT \quad (5)$$

where G is the Gibbs energy function and H is the enthalpy. This provides the location of the melting point of the quantum system as the temperature at which the chemical potential of ice I_h and water become identical.

2.2 Calculation of the TMD

The determination of the location of the TMD consisted in particularly long simulation runs (up to 9 million Monte Carlo cycles per temperature) for a range of temperatures that bracket the location of the TMD. Once the densities as a function of temperature were obtained, they were fitted to a quadratic polynomial, whose maxima was taken to be the location of the TMD.

3 Results

3.1 Melting point of the TIP4PQ/2005 model

The classical value of the melting point for the TIP4PQ/2005 was calculated to be 282K¹¹. As per Step 2 of the methodology outlined previously, the integrand of equation 1 was calculated and the results are presented in Figure 1.

One can see that this integrand is positive, indicating that the molecules have more kinetic energy in the ice phase than they

Model	T (K)	$\Delta\mu(I_h - \text{liquid}) / (k_B T)$
TIP4PQ/2005	282	0.198
TIP4PQ/2005 (D ₂ O)	282	0.120
TIP4PQ/2005 (T ₂ O)	282	0.092
TIP4PQ_D2O	276	0.108
TIP4PQ_T2O	273	0.084

Table 3 The difference in the chemical potential between the ice and liquid phases in the quantum system, evaluated at the T_m of the classical system at a pressure of $p = 1$ bar. (Error ± 0.01).

Model	T_m	$T_m - T_m^{H_2O}$	T_{TMD}	$T_{TMD} - T_{TMD}^{H_2O}$
H ₂ O (experiment)	273.15	0	277.13	0
D ₂ O (experiment)	276.83	3.68	284.34	7.2
T ₂ O (experiment)	277.64	4.49	286.55	9.4
	T_m	$T_m - T_m^{\text{TIP4PQ/2005}}$	T_{TMD}	$T_{TMD} - T_{TMD}^{\text{TIP4PQ/2005}}$
TIP4PQ/2005	258.3	0	284	0
TIP4PQ/2005 (D ₂ O)	267.7	9.4	295	11
TIP4PQ/2005 (T ₂ O)	271.8	13.5	300	16
TIP4PQ/2005	258.3	0	284	0
TIP4PQ_D2O	263.2	4.9	290	6
TIP4PQ_T2O	263.5	5.2	291	7

Table 4 Melting points and temperatures of maximum density of the models (all temperatures are in Kelvin).

do in the liquid phase, thus ice I_h is less stable in the quantum system, which in turn implies that the melting point will move to lower temperatures in the quantum system. Since the hydrogen bonds are stronger in the ice phase quantum effects are more influential in the ice phase. The integrand is fairly smooth, and so can be fitted to a straight line down to very small values of λ' , and it is from this fit that we obtain the value of the integral. The values for these integrals are presented in Table 3. Having these integrals we proceeded to Step 3, i.e. the thermodynamic integration given in Eq. 5. To do this path integral simulations were performed for both ice I_h and water at various temperatures along the $p = 1$ bar isobar. The melting point of the quantum system is the temperature at which the chemical potential of both I_h and water are the same. The resulting melting points are given in Table 4.

The melting point of the TIP4PQ/2005 model is 258K, which is approximately 15K below the experimental value. TIP4PQ/2005 is not alone in underestimating the melting point; the flexible q-TIP4P/F model¹², also designed for use in path integral simulations, has a similar melting point (251 K²⁶). This is probably due to the fact that both the q-TIP4P/F and TIP4PQ/2005 models are derived from the classical TIP4P/2005 model which has $T_m = 252$ K. The TTM2.1-F and TTM3-F models²⁷, which are both flexible and polarisable and were obtained from fits to high level *ab initio* calculations, have somewhat lower melting points; 228 K²⁸ and 225 K²⁹ respectively, while the q-SPC/Fw model³⁰ has a T_m of 195

K¹². Conversely, density functional theory predictions for the melting point tend to significantly overestimate the experimental value; two common functionals, PBE0 and BLY3P,³¹ have a melting point of $T_m = 415$ K.

From Table 5 one can see that the TIP4PQ/2005 models underestimate the melting enthalpy (1.099 kcal/mol, whereas the experimental value is 1.436 kcal/mol). The enthalpy of melting was obtained from *NpT* simulations of both the solid phase and the liquid phase, for each model, both at the melting point, then simply taking the enthalpy difference at this temperature. Both of these results, the melting point and the melting enthalpy, were also underestimated in classical simulations of the classical model TIP4P/2005 (251 K and 1.15 kcal/mol respectively). From this we can deduce that the inclusion of nuclear quantum effects has relatively little influence over these properties, and that any discrepancy with experiment is due to the approximate description of the PES implied in the empirical TIP4P/2005 and TIP4PQ/2005 models.

3.2 Isotope effects on the melting point

In classical simulations the melting point is independent of the molecular mass, thus the melting points of the TIP4PQ/2005 (D₂O) and TIP4PQ/2005 (T₂O) models is the same as that of the TIP4PQ/2005 model, namely 282K. As per Step 2 of the methodology outlined previously the integrand of equation 1 was calculated (see Figure 1) and the integral of Eq.(1) eval-

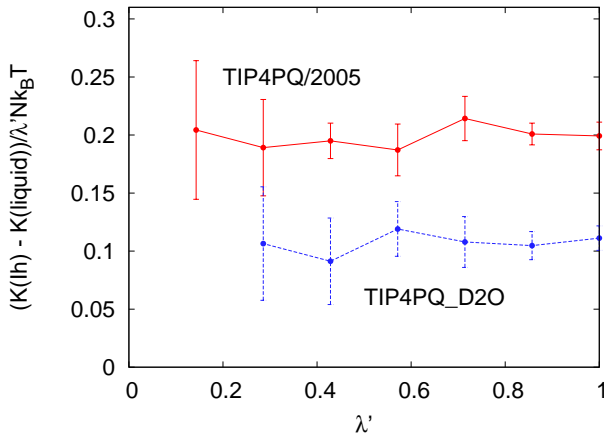


Figure 1 Integrand of Eq. 1 (i.e. $(K_{Ih} - K_{\text{liquid}})/(\lambda' N k_B T)$) as a function of λ' . The integral of the curves (from 0 to 1) yields $\Delta\mu(I_h - \text{liquid})/(k_B T)$. Key: TIP4PQ/2005 red line, TIP4PQ_D2O blue dashed line.

uated (see Table 3). Thermodynamic integration was then undertaken leading to the melting points of the quantum system; 268K for TIP4PQ/2005 (D_2O) and 272K for TIP4PQ/2005 (T_2O). This increase in the melting point qualitatively mirrors experimental results, however, the magnitude of the shift is over estimated (see column 3 of Table 4).

The same procedure was applied to the TIP4PQ_D2O and TIP4PQ_T2O models, which have classical melting points of 276 K and 273 K respectively. We find a difference of 4.9 K between TIP4PQ_D2O and TIP4PQ/2005, and 5.2 K between TIP4PQ_T2O and TIP4PQ/2005, which is in much better agreement with the experimental value of the shift. Similar values for the melting point differences were found for the q-TIP4P/F model; 6.5K between D_2O and H_2O , and 8.2 for T_2O with respect to H_2O ³². For D_2O the melting enthalpy is found to be from experiments about 0.07 kcal/mol higher than that of water, whereas TIP4PQ/2005 predicts an increase of 0.09 kcal/mol and TIP4PQ_D2O predicts an increase of about 0.04 kcal/mol.

3.3 Isotope effects on the temperature of maximum density (TMD)

Experimentally deuteration of water shifts the TMD by 7.2 K³³, and tritiation by 9.4 K³⁴. Our previous results³⁵ indicate that deuteration and tritiation of the TIP4PQ/2005 model tended to overestimate this shift. Our new models now slightly underestimate this shift (see Table 4 and figure 2). In view of the fact that the error bar for the TMD is fairly large (± 2 K), these results are reasonable. Especially when one bears in mind

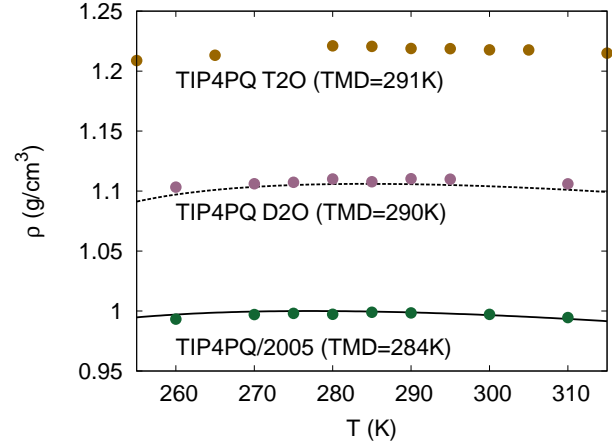


Figure 2 Plot of the isobars ($p = 1$ bar) used to calculate the TMD (points), along with fits to experimental results³⁷ for H_2O and D_2O (lines) (the authors were unable to locate experimental data for T_2O).

that an isotopic shift in the TMD is not always present in a number of recent models^{32,36}, as is the case of the q-TIP4P/F¹² and the TTM2.1-F models.

3.4 The temperature difference between the melting point and the TMD

Of particular interest is the difference between the TMD and T_m . Experimentally this difference is 3.98 K for H_2O , 7.5 K for D_2O , and 8.9 K for T_2O . From our simulations we obtain 25.7 K for TIP4PQ/2005, 26.8 K for TIP4PQ_D2O and 27.5 K for TIP4PQ_T2O. As can be seen all the models presented in this work are unable to describe the difference between the temperature of the TMD and the melting point temperature. Thus the inclusion of nuclear quantum effects does not solve the disagreement with experiment indicating that the origin of this failure is the approximate character of the PES. The same is true for the q-TIP4P/F which predicts a difference between the TMD and the melting point of 26 K (the model has the TMD at 277 K and the melting point at 251 K). For the TTM2.1-F models³⁸ the difference between the TMD and the melting point is even higher (45 K) (the melting point is located at 228 K²⁸ and the TMD at 273 K²⁷). One can conclude that no model designed for path integral simulations thus far is able to reproduce the difference between the TMD and the melting point found experimentally.

3.5 Isotope effects on molar volumes

Bridgman described that the “*molar volume of D_2O is always greater than that of H_2O at the same pressure and tempera-*

Model	$\Delta H(T_m)$ (kcal/mol)	$\rho_{I_h}(T_m)$	$\rho_{\text{liquid}}(T_m)$
H ₂ O (experiment)	1.436	0.917	0.999
D ₂ O (experiment)	1.509	1.018	1.105
T ₂ O (experiment)	—	—	—
TIP4PQ/2005	1.099	0.919	0.988
TIP4PQ/2005 (D ₂ O)	1.189	1.028	1.103
TIP4PQ/2005 (T ₂ O)	1.285	1.134	1.212
TIP4PQ_D2O	1.133	1.024	1.091
TIP4PQ_T2O	1.192	1.128	1.214

Table 5 The change in enthalpy at the melting points of the models along with densities in units of g/cm³ (experimental values from IAPWS-95/NIST Standard Reference Data).

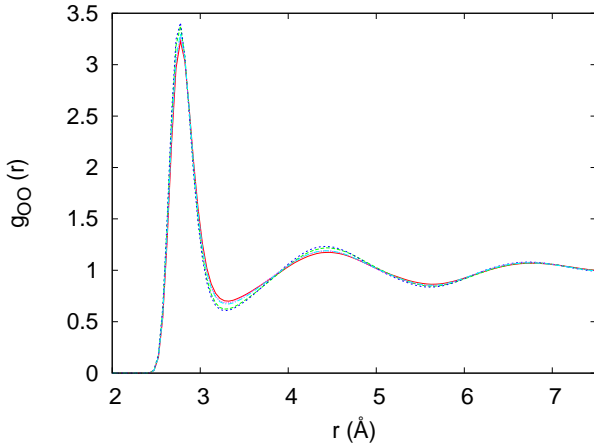


Figure 3 Plot of the O-O radial distribution function for water at 290 K and $p = 1$ bar. Key: TIP4PQ/2005 red line, TIP4PQ/2005 (D₂O) dashed green line, TIP4PQ/2005 (T₂O) dashed blue line, TIP4PQ_D2O dotted pink line and TIP4PQ_T2O dot-dashed cyan line.

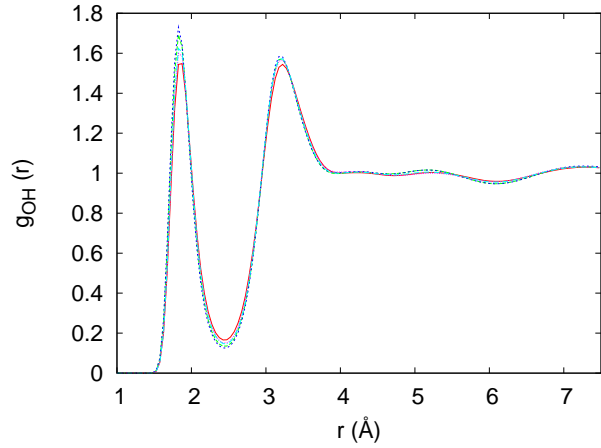


Figure 4 Plot of the O-H radial distribution function for water at 290 K and $p = 1$ bar. The same key as in Fig. 3.

3.6 Isotope effects on the structure

In Figures 3-5 we provide the atom-atom distribution functions for O-O, H-H and O-H for each of the models studied. From these plots, whose salient features are compiled in Table 6, one can observe that the structure of the new models, TIP4PQ_D2O and TIP4PQ_T2O is very similar to that of TIP4PQ/2005, more so than that of TIP4PQ/2005 (D₂O) and TIP4PQ/2005 (T₂O). This implies that the structure of the fluid phase of isotopically substituted water is almost indistinguishable from that of H₂O, an assumption that experimentalists often make, and one that seems to be justified by our simulation results.

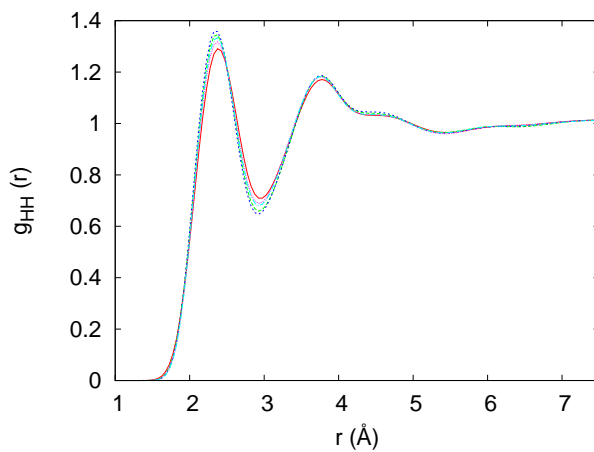
3.7 Isotope effects on the diffusion coefficient

In the work of Habershon et al.¹² a H₂O/D₂O diffusion coefficient ratio of 1.28 was found for the q-TIP4P/F model at 298K (experimentally it is 1.30). Although it is not possible to directly compute the diffusion coefficient from Monte

ture”³⁹. Experimentally for ice I_h this difference was seen to be of the order of 0.2% at 220K^{40,41}. From our simulations of ice I_h we obtained 32.410 Å³/molecule for TIP4PQ/2005 at 220K, and 32.303 Å³/molecule for TIP4PQ_D2O, also at 220K, which is similar to experimental results of 32.367 and 32.429 for H₂O and D₂O respectively⁴², also at 220K. From this one can see that the models used here are unable to capture this (albeit subtle) effect. However, recent *ab initio* density functional theory calculations have been able to reproduce this effect⁴², although there is a ≈ 4% error in the densities themselves. It would be interesting to see whether *ab initio* density functional theory calculations are also capable of reproducing the isotopic shifts found in the T_m and the TMD.

Table 6 O-O, O-H and H-H radial distribution function of water for the various models at 290 K and $p = 1$ bar.

Model	peak 1		peak 2	
	r (Å)	height	r (Å)	height
TIP4PQ/2005	2.775	3.23	4.475	1.17
TIP4PQ/2005 (D_2O)	2.775	3.38	4.425	1.22
TIP4PQ/2005 (T_2O)	2.775	3.41	4.425	1.23
TIP4PQ_D2O	2.775	3.27	4.425	1.19
TIP4PQ_T2O	2.775	3.30	4.425	1.19
TIP4PQ/2005	1.875	1.55	3.225	1.54
TIP4PQ/2005 (D_2O)	1.825	1.69	3.225	1.57
TIP4PQ/2005 (T_2O)	1.825	1.73	3.175	1.58
TIP4PQ_D2O	1.825	1.60	3.225	1.57
TIP4PQ_T2O	1.825	1.62	3.225	1.57
TIP4PQ/2005	2.375	1.29	3.775	1.17
TIP4PQ/2005 (D_2O)	2.375	1.34	3.775	1.18
TIP4PQ/2005 (T_2O)	2.375	1.36	3.775	1.19
TIP4PQ_D2O	2.375	1.32	3.775	1.18
TIP4PQ_T2O	2.375	1.33	3.775	1.18

**Figure 5** Plot of the H-H radial distribution function for water at 290 K and $p = 1$ bar. The same key as in Fig. 3.

Carlo runs, a rough estimate can be obtained by calculating the mean square displacement of the molecules after a fixed number of Monte Carlo cycles. In our simulations the ratio of the mean square displacement (after 200,000 MC cycles) between TIP4PQ/2005 and TIP4PQ/2005 (D_2O), was 1.33. When we compare TIP4PQ/2005 with TIP4PQ_D2O we obtain a ratio of 1.17, indicating that the new model decreases the differences between D_2O and H_2O , in line with the results for the radial distribution function.

3.8 Heat capacity C_p

The isobaric heat capacity was obtained from a differential of the enthalpy with respect to temperature. At 280K the values we obtained were (in cal/mol/K) TIP4PQ/2005 17.4, TIP4PQ_D2O 18.7 and for TIP4PQ_T2O 19.5. These results compare favourably with the experimental values; H_2O is 17.9⁴³ and D_2O is 20.3⁴⁴.

4 Conclusions

We have seen the “competing quantum effects” interpretation of Habershon et al. in action; the TIP4PQ/2005, TIP4PQ/2005 (D_2O) and TIP4PQ/2005 (T_2O) models all have the same geometry and charge distribution, thus they all have the same dipole moment. When one examines the radial distribution functions one can see that the TIP4PQ/2005 (D_2O) and TIP4PQ/2005 (T_2O) models have stronger features than the TIP4PQ_D2O and TIP4PQ_T2O models, whose dipole moments are smaller. The new models presented here for D_2O and T_2O were designed by shortening the O-H bond length in line with the values presented by Zeidler et al.¹⁵. It is worth noting that a bond length reduction by as much as 4%, as suggested by Soper and Benmore⁴⁵, would probably have led to a significant error in our evaluation the isotopic influence on the melting point. We have seen that the models studied in this work underestimate the melting point by $\approx 7\%$ and the melting enthalpy by $\approx 30\%$. This is almost certainly due to the approximate nature of the empirical potentials used here, failing to reproduce the experimental PES. The situation is more

favourable when one considers isotopic shifts. In general we have seen that the models qualitatively reproduce the experimental trends. The models proposed in this work for D₂O and T₂O predict an increase both in the TMD and in the melting point which are more realistic than those predicted by isotopic substitution in the TIP4PQ/2005 models.

This work was funded by grants FIS2010-16159 and FIS2010-15502 of the Dirección General de Investigación and S2009/ESP-1691-QF-UCM (MODELICO) of the Comunidad Autónoma de Madrid. One of the authors (J. L. A.) would like to thank the MEC for a FPI pre-doctoral studentship. The authors would like to thank Prof. Jose Luis Abascal for many helpful discussions.

References

- [1] A. Wallqvist and B. J. Berne, *Chem. Phys. Lett.*, 1985, **117**, 214.
- [2] R. A. Kuharski and P. J. Rossky, *Chem. Phys. Lett.*, 1984, **103**, 357.
- [3] M. J. Gillan, in *The path-integral simulation of quantum systems*, ed. C. R. A. Catlow, S. C. Parker and M. P. Allen, Kluwer, The Netherlands, 1990, vol. 293, ch. 6, pp. 155–188.
- [4] K.-Y. Wong, in *Developing a Systematic Approach for Ab Initio Path-Integral Simulations*, ed. L. Wang, InTech, 2012, ch. 6, p. 107.
- [5] B. Guillot, *J. Molec. Liq.*, 2002, **101**, 219.
- [6] C. Vega and J. L. F. Abascal, *Phys. Chem. Chem. Phys.*, 2011, **13**, 19663.
- [7] J. L. F. Abascal and C. Vega, *J. Chem. Phys.*, 2005, **123**, 234505.
- [8] L. H. de la Peña, M. S. G. Razul and P. G. Kusalik, *J. Chem. Phys.*, 2005, **123**, 144506.
- [9] E. Curotto, D. L. Freeman and J. D. Doll, *J. Chem. Phys.*, 2008, **128**, 204107.
- [10] C. McBride, C. Vega, E. G. Noya, R. Ramírez and L. M. Sesé, *J. Chem. Phys.*, 2009, **131**, 024506.
- [11] C. McBride, E. G. Noya, J. L. Aragones, M. M. Conde and C. Vega, *Phys. Chem. Chem. Phys.*, 2012, **14**, 10140.
- [12] S. Habershon, T. E. Markland and D. E. Manolopoulos, *J. Chem. Phys.*, 2009, **131**, 024501.
- [13] T. Lu, G. Tth and K. Heinzinger, *J. Phys. Chem.*, 1996, **100**, 1336.
- [14] Q. Waheed and O. Edholm, *Journal of Chemical Theory and Computation*, 2011, **7**, 2903.
- [15] A. Zeidler, P. S. Salmon, H. E. Fischer, J. C. Neufeind, J. M. Simonson, H. Lemmel, H. Rauch and T. E. Markland, *Phys. Rev. Lett.*, 2011, **107**, 145501.
- [16] J. L. F. Abascal and C. Vega, *Phys. Rev. Lett.*, 2007, **98**, 237801.
- [17] E. G. Noya, L. M. Sesé, R. Ramírez, C. McBride, M. M. Conde and C. Vega, *Molec. Phys.*, 2011, **109**, 149.
- [18] E. G. Noya, C. Vega and C. McBride, *J. Chem. Phys.*, 2011, **134**, 054117.
- [19] M. H. Müser and B. J. Berne, *Phys. Rev. Lett.*, 1996, **77**, 2638.
- [20] J. D. Bernal and R. H. Fowler, *J. Chem. Phys.*, 1933, **1**, 515.
- [21] V. Buch, P. Sandler and J. Sadlej, *J. Phys. Chem. B*, 1998, **102**, 8641.
- [22] L. Pauling, *J. Am. Chem. Soc.*, 1935, **57**, 2680.
- [23] C. Vega, E. Sanz, J. L. F. Abascal and E. G. Noya, *J. Phys. Cond. Mat.*, 2008, **20**, 153101.
- [24] P. J. Mohr, B. N. Taylor and D. B. Newell, *Rev. Modern Phys.*, 2008, **80**, 633.
- [25] R. G. Fernández, J. L. F. Abascal and C. Vega, *J. Chem. Phys.*, 2006, **124**, 144506.
- [26] S. Habershon and D. E. Manolopoulos, *Phys. Chem. Chem. Phys.*, 2011, **13**, 19714.
- [27] G. S. Fanourgakis and S. S. Xantheas, *J. Chem. Phys.*, 2008, **128**, 074506.
- [28] F. Paesani and G. A. Voth, *The Journal of Physical Chemistry C*, 2008, **112**, 324.
- [29] F. Paesani, S. Yoo, H. J. Bakker and S. S. Xantheas, *J. Phys. Chem. Lett.*, 2010, **1**, 2316.
- [30] F. Paesani, W. Zhang, D. A. Case, T. E. Cheatham III and G. A. Voth, *J. Chem. Phys.*, 2006, **125**, 184507.
- [31] S. Yoo, X. C. Zeng and S. S. Xantheas, *J. Chem. Phys.*, 2009, **130**, 221102.
- [32] R. Ramírez and C. P. Herrero, *J. Chem. Phys.*, 2010, **133**, 144511.
- [33] P. G. Hill, R. D. C. MacMillan and V. Lee, *J. Phys. Chem. Ref. Data*, 1982, **11**, 1.
- [34] F. Franks, *Water: A Matrix of Life*, RSC Publishing, 2nd edn, 2000.
- [35] E. G. Noya, C. Vega, L. M. Sesé and R. Ramírez, *J. Chem. Phys.*, 2009, **131**, 124518.
- [36] F. Paesani, S. Iuchi and G. A. Voth, *J. Chem. Phys.*, 2007, **127**, 074506.
- [37] V. S. Kravchenko, *Atomic Energy*, 1966, **20**, 168.
- [38] G. S. Fanourgakis and S. S. Xantheas, *J. Phys. Chem. A*, 2006, **110**, 4100.
- [39] P. W. Bridgman, *J. Chem. Phys.*, 1935, **3**, 597.
- [40] K. Röttger, A. Endriss, J. Ihringer, S. Doyle and W. F. Kuhs, *Acta Crystallographica Section B Structural Science*, 1994, **50**, 644.
- [41] K. Röttger, A. Endriss, J. Ihringer, S. Doyle and W. F. Kuhs, *Acta Crystallographica Section B Structural Science*, 2012, **68**, 91.
- [42] B. Pamuk, J. M. Soler, R. Ramírez, C. P. Herrero, P. W. Stephens, P. B. Allen and M. V. Fernández-Serra, *Phys. Rev. Lett.*, 2012, **108**, 193003.
- [43] C. A. Angell, W. J. Sichina and M. Oguni, *J. Phys. Chem.*, 1982, **86**, 998.
- [44] A. Braibanti, E. Fisicaro, A. Ghiozzi and C. Compari, *Thermochimica Acta*, 1996, **286**, 51.
- [45] A. K. Soper and C. J. Benmore, *Phys. Rev. Lett.*, 2008, **101**, 065502.